yes

Los Alamos

Los Alamos National Laboratory
Los Alamos, New Mexico 87545

memorandum

TO: Distribution

DATE: 10 February, 1987

FROM: Mike Fehler, ESS-4 MJ

MAIL STOP/TELEPHONE: J979/7-1925

SYMBOL: ESS-4-87-32

SUBJECT: Application of the three point method to experiment 2032: Results

The three point method is a method that I have developed over the past year for looking for patterns (planes) in the microearthquake location data collected during hydraulic fracturing experiments. I have prepared a complete paper for publication (in the Journal of Geophysical Research) that describes the method and the results of applying the method to data collected during experiment 2032 (THE MHF). I distributed a preliminary version of this paper to some of you. The paper has been reviewed by the journal and the reviewers suggested many helpful improvements which I have now made (both in the paper and some modifications to the method). The paper is now modified. I will be happy to provied the current version of the paper to anyone who wants it but am not distributing it to everyone since it would require lots of trees to loose their lives. This memo is a summary of the results of applying the method to experiment 2032 and avoids all the detail of how I got the results to be presented. I hope that this memo will generate discussion of the usefulness of the method as applied to hydraulic fracturing data.

I iteratively applied the method to the 2032 data and successfully determined the orientations and locations of 5 planes or sets of planes along which the earthquakes fall. The dataset consisted of 844 quality a and b locations (Leigh House's location set 3, which we have used for all of our interpretation of this experiment). The method was applied to find the location and orientation of one plane. The earthquakes that fall along this plane were then eliminated from the dataset and the method was reapplied to determine if another plane could be found. This was repeated until no planes passed a statistical significance test (basically requires that there be less than a 1 in 10000 chance that the result could be caused by random chance). Table 1 (from the full paper) is a list of important parameters for the 5 planes. I consider the first three planes to be extremely reliable, the last two are perhaps less so.

Figure 1 is a plot showing how perfect data would look if it fell along the first plane found by the method, which is shown in figure 2. The upper map in figure 1 is a vertical cross section looking towards N31W, parallel to the strike of the plane. For this map, I chose 101 events to fall at random locations along a plane that strikes N31W and dips 74°E. The data are artificial. The lower part of the figure shows how the data look if I perturb each location in the upper part of the figure. This has been done in an attempt to show how the data might look if there are errors in locations. In this case, I have perturbed each location in a random direction from its original location in such a way that the mean of the perturbations is 0 and the standard deviation is 20m, or approximately the amount of relative error that we estimate that our 2032 locations contain. It can be seen that the width of the zone is quite large in the presence of error. To test the three point method I added 743 locations to these 101 locations, making a total of 844 locations, and applied the three point method to see if I could find this plane. The 743 locations were spread throughout the 2032 seismic zone. The three point method successfully located this plane in the noisy data. In fact, if I perturbed the locations by as much as 50m, the method was still successful at determining the location and orientation of the plane. Since we estimate our locational precision to be 20m, the above test is a good indication of the reliability of the method when applied to the 2032 data.

In order to show the locations of the planes, I have prepared three orthogonal views of the locations of the events that fall along each plane. These are shown in figures 2-6. The three orthogonal views are a map view, a vertical cross section looking parallel to the plane and a vertical cross section looking face on to the plane. Note that the view direction of the vertical cross sections are necessarily different for each plane. The direction in which the viewer is looking for each cross section is listed below the map. In addition, there is an eye showing the direction that the viewer is looking.

Comparing the vertical cross section looking towards N31W (labeled as -031) we see that the width of the seismic zone that defines the main plane is approximately the same as the width of the zone shown in the lower map in figure 1. This shows some agreement between our estimate of the relative location errors and the result of the three point method. The center of the plane intersects EE-2 at a depth of 3520m true vertical depth (TVD), 11825 feet depth along wellbore (DAW), in a region where fractures that took water in experiments 2018 and 2020 were found. Some of these fractures were sanded in prior to experiment 2032. According to my notes, the top of the sand is at 3500 m TVD or 11,650 feet DAW.

The second plane, shown in figure 3, intersects the EE-3a wellbore at a depth of 3770 m TVD, 11610 feet DAW from Kelly bushing, in a region near to where Schon Levy finds abundant fractures in the cuttings from EE-3a. Note that this plane intersects the EE-3a wellbore although the water was injected into EE-2. EE-3a did not exist at the time that this water was injected.

Figure 7 shows lower hemisphere projections of the fault plane solutions that occurred most frequently in experiment 2032. These were obtained by Leigh House in a study of the data made by redigitizing all surface network events on the Masscomp. The solid lines show the traces of the two nodal planes for each of the two soultions. The nodal planes define the plane along which slip occurred. In performing the fault plane solution, we have no means by which we can choose which of the two planes is the correct plane along which slip occurred. The dotted lines show the traces of the first two planes (from figures 2 and 3) found by the three point method. The first plane found is parallel to one of the two nodal planes for the left hand fault plane solution in Figure 7. The second plane is parallel to one of the two nodal planes for the right hand fault plane solution. This means that we now know which of the two nodal planes was the slip plane for each fault plane solution.

Distribution

J. Whetten, A107
D. Evans D446
W. Myers D446
S. Levy D462
B. Laughlin D462
All ESS-4
All ESS-6
All HDR ESS-DOT

ESS-4 File

TABLE 1. PLANES DETERMINED BY APPLICATION OF THE THREE POINT METHOD

Plane Strike	Plane Dip	Number of Events on Plane	Number of Standard Deviations above Mean
N31W	74E	130	11.4
N90W	27N	35	6.8
N29W	67W	50	6.1
N7E	67E	81	5.8
N29E	60W	28	4.1

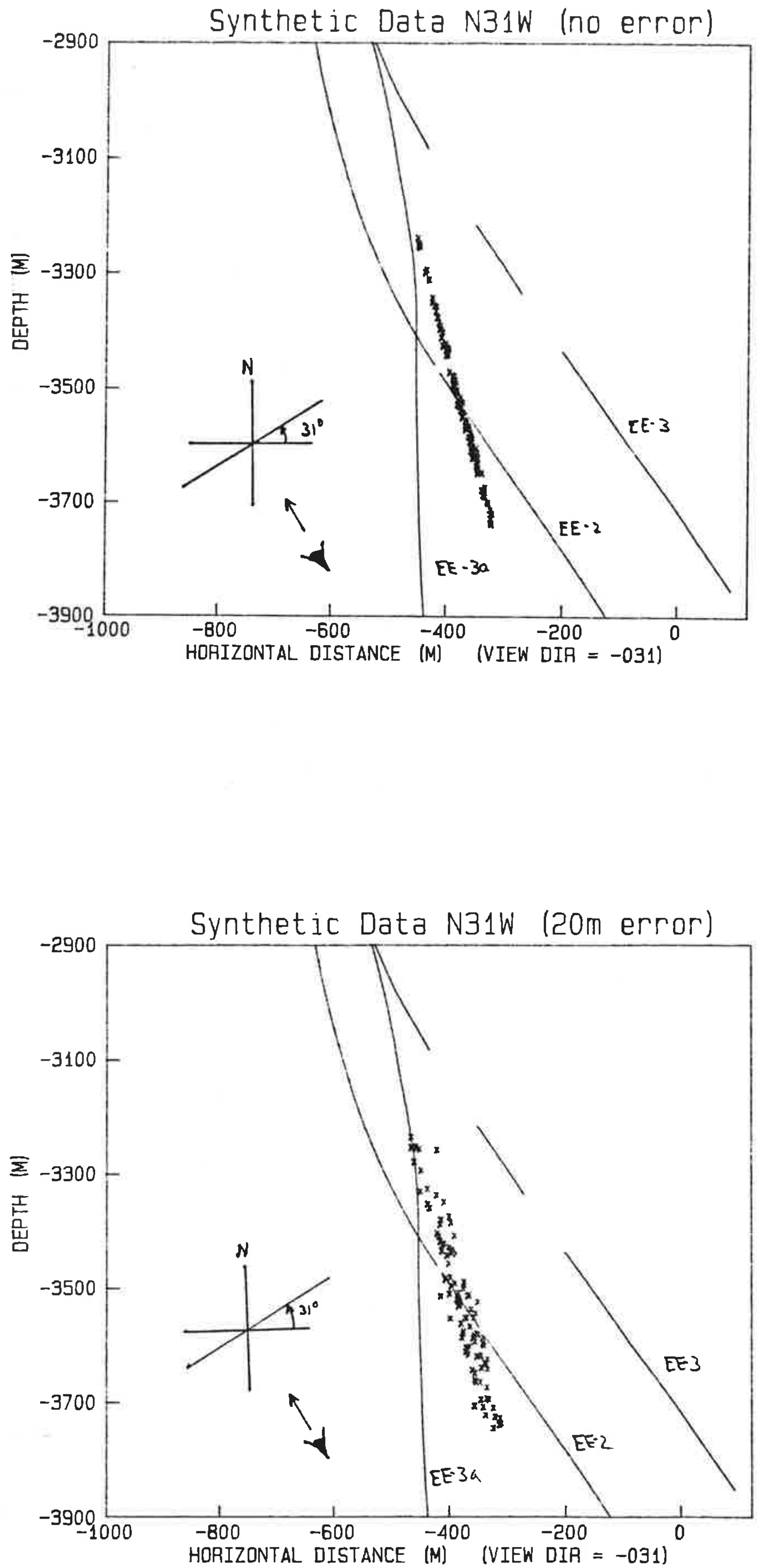
Synthetic Data N31W (no error)
-2900
-3100
-3300
-3500
-3700
-3900
DEPTH (M)
-1000
-800
-600
-400
-200
0
HORIZONTAL DISTANCE (M) (VIEW DIR = -031)
N
31°
EE-3
EE-2
EE-3a
Synthetic Data N31W (20m error)
-2900
-3100
-3300
-3500
-3700
-3900
DEPTH (M)
-1000
-800
-600
-400
-200
0
HORIZONTAL DISTANCE (M) (VIEW DIR = -031)
N
31°
EE3
EE2
EE3a

Figure 1

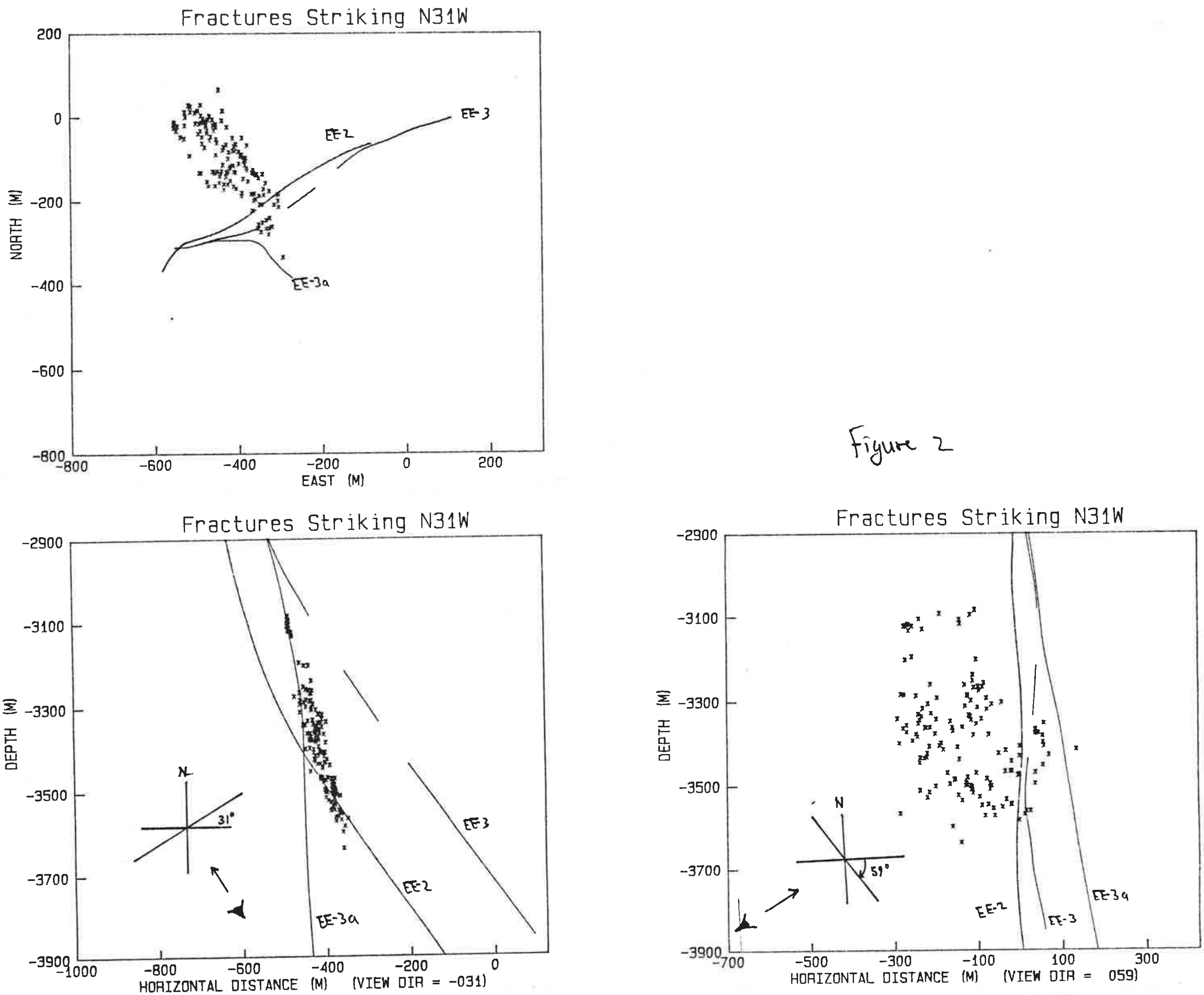
Fractures Striking N31W
NORTH (M)
EAST (M)
EE-3
EE-2
EE-3a
Fractures Striking N31W
DEPTH (M)
HORIZONTAL DISTANCE (M) (VIEW DIR = -031)
N
31°
EE-3
EE-2
EE-3a
Fractures Striking N31W
DEPTH (M)
HORIZONTAL DISTANCE (M) (VIEW DIR = 059)
N
59°
EE-2
EE-3
EE-3a

Figure 2

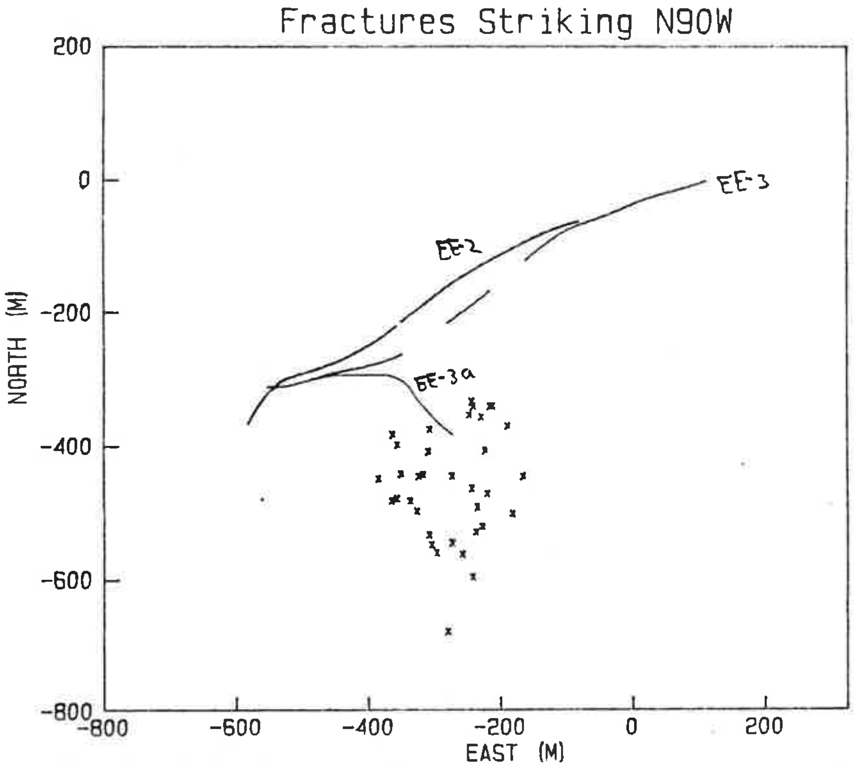
Fractures Striking N90W
NORTH (M)
EAST (M)
200
0
-200
-400
-600
-800
-800
-600
-400
-200
0
200
EE-2
EE-3
EE-3a

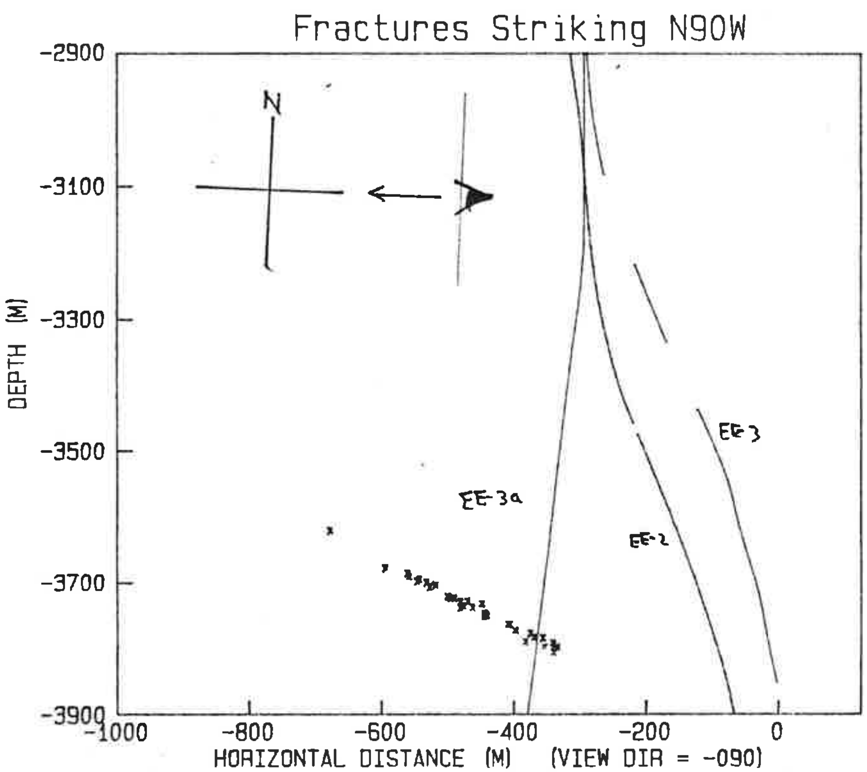
Fractures Striking N90W
DEPTH (M)
HORIZONTAL DISTANCE (M) (VIEW DIR = -090)
-2900
-3100
-3300
-3500
-3700
-3900
-1000
-800
-600
-400
-200
0
N
EE-3a
EE-2
EE-3

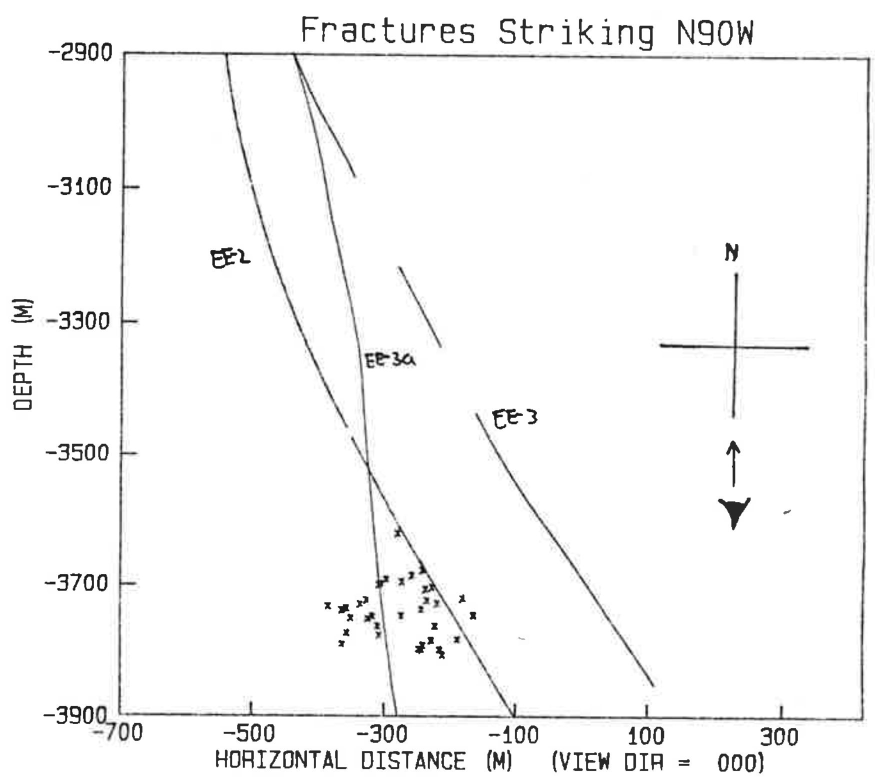
Fractures Striking N90W
DEPTH (M)
HORIZONTAL DISTANCE (M) (VIEW DIR = 000)
-2900
-3100
-3300
-3500
-3700
-3900
-700
-500
-300
-100
100
300
N
EE-2
EE-3a
EE-3

Figure 3

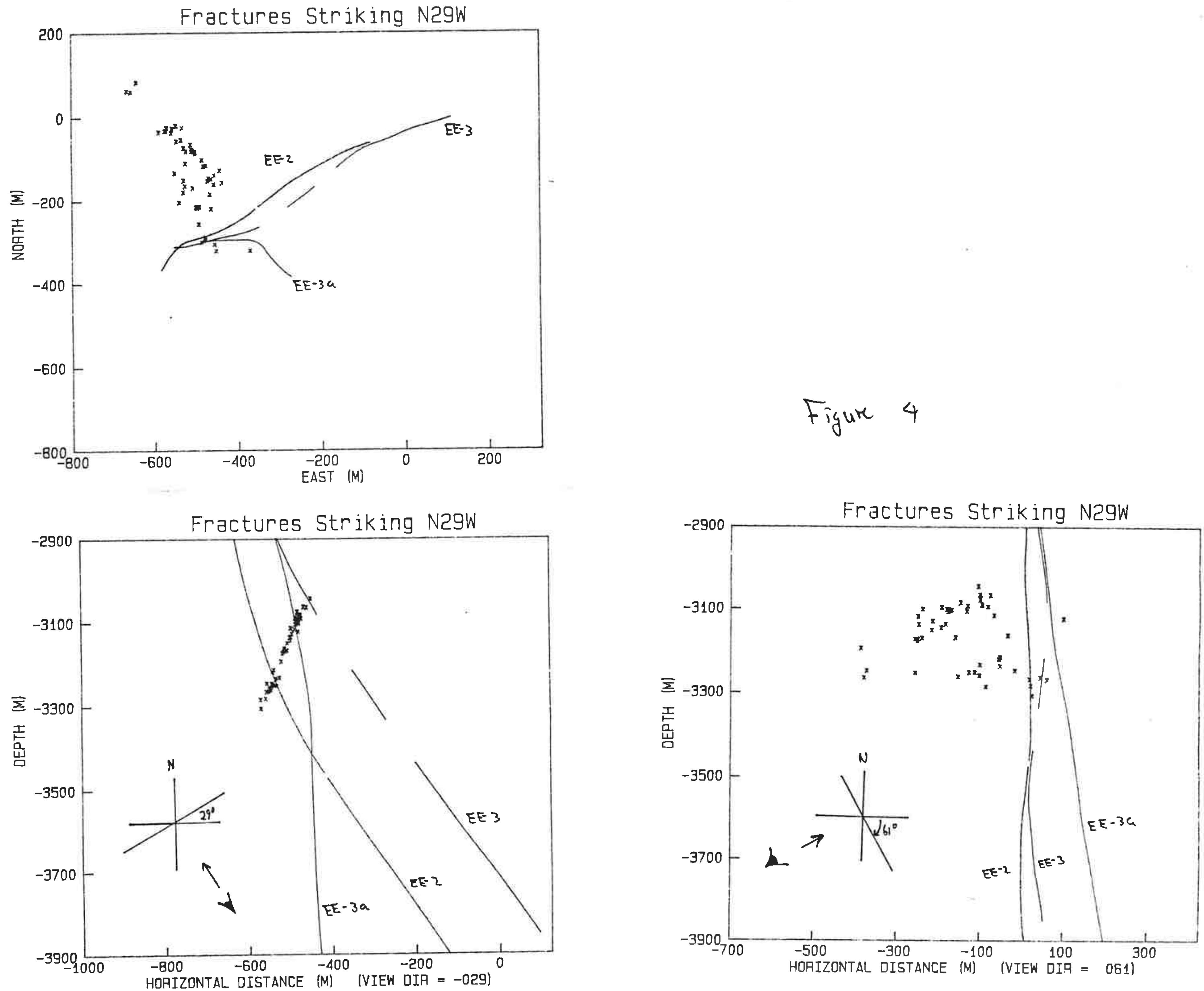
Fractures Striking N29W
NORTH (M)
EAST (M)
200
0
-200
-400
-600
-800
-800
-600
-400
-200
0
200
EE-2
EE-3
EE-3a
Fractures Striking N29W
DEPTH (M)
HORIZONTAL DISTANCE (M) (VIEW DIR = -029)
-2900
-3100
-3300
-3500
-3700
-3900
-1000
-800
-600
-400
-200
0
N
29°
EE-3a
EE-2
EE-3
Fractures Striking N29W
DEPTH (M)
HORIZONTAL DISTANCE (M) (VIEW DIR = 061)
-2900
-3100
-3300
-3500
-3700
-3900
-700
-500
-300
-100
100
300
N
61°
EE-2
EE-3
EE-3a

Figure 4

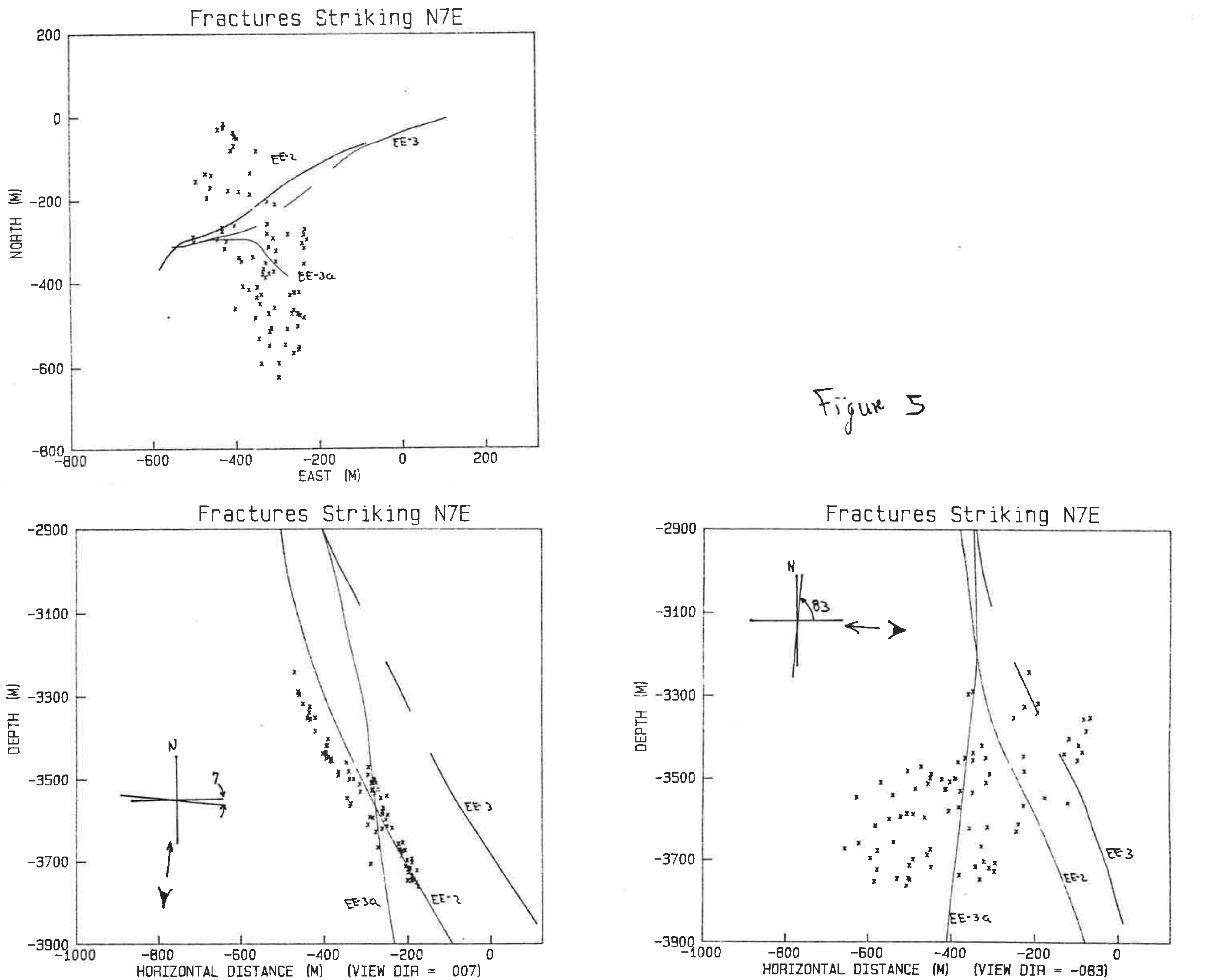
Fractures Striking N7E
NORTH (M)
EAST (M)
EE-2
EE-3
EE-3a
Fractures Striking N7E
DEPTH (M)
HORIZONTAL DISTANCE (M) (VIEW DIR = 007)
N
7
EE-3
EE-2
EE-3a
Fractures Striking N7E
DEPTH (M)
HORIZONTAL DISTANCE (M) (VIEW DIR = -083)
N
83
EE-3
EE-2
EE-3a

Figure 5

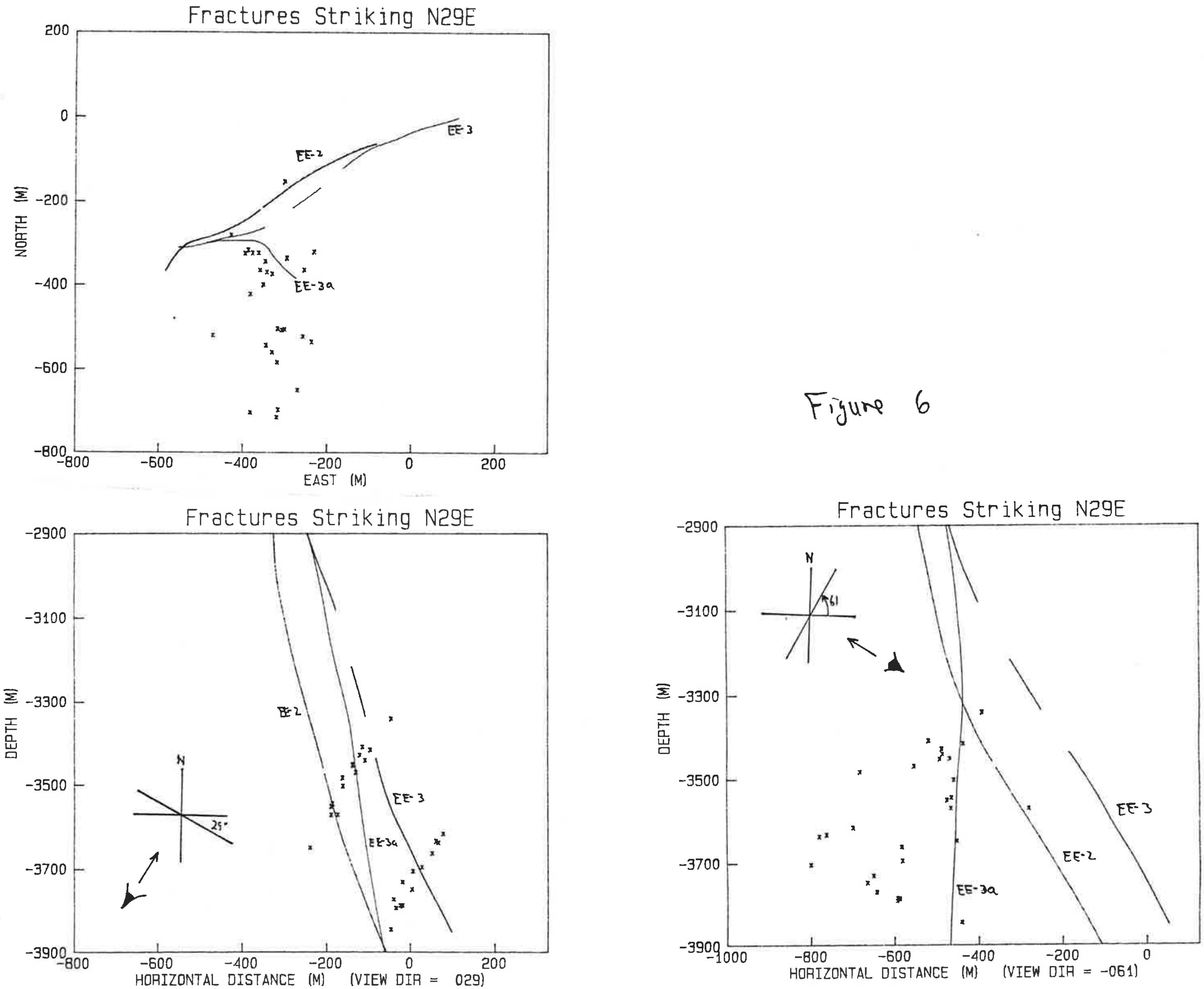
Fractures Striking N29E
NORTH (M)
EAST (M)
EE-2
EE-3
EE-3a
Fractures Striking N29E
DEPTH (M)
HORIZONTAL DISTANCE (M) (VIEW DIR = 029)
N
25°
EE-2
EE-3
EE-3a
Fractures Striking N29E
DEPTH (M)
HORIZONTAL DISTANCE (M) (VIEW DIR = -061)
N
61
EE-2
EE-3
EE-3a

Figure 6

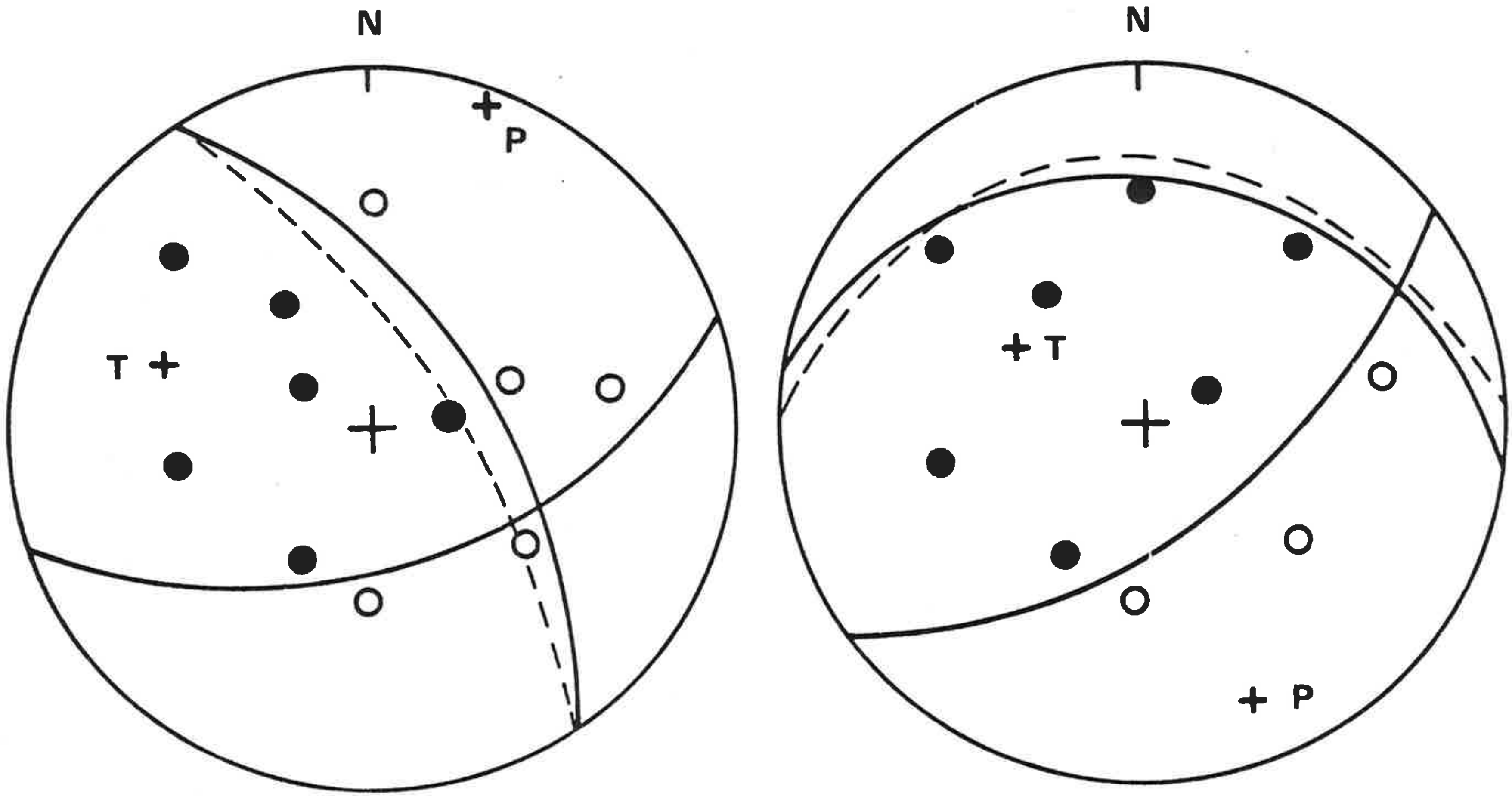

Figure 7